Computers and Electronics in Agriculture 118 (2015) 100–110

Contents lists available at ScienceDirect

Computers and Electronics in Agriculture

journal homepage: www.elsevier.com/locate/compag

Original papers

A strategy to simulate radio frequency heating under mixing conditions

Long Chen [a], Kun Wang [a], Wei Li [a], Shaojin Wang [a,b,*]

[a] College of Mechanical and Electronic Engineering, Northwest A&F University, Yangling, Shaanxi 712100, China
[b] Department of Biological Systems Engineering, Washington State University, Pullman, WA 99164-6120, USA

ARTICLE INFO

Article history:
Received 5 February 2015
Received in revised form 21 August 2015
Accepted 22 August 2015

Keywords:
RF heating
Wheat sample
Computer simulation
Mixing
Heating uniformity

ABSTRACT

A computer simulation model was developed using finite element-based commercial software, COMSOL, to simulate temperature distributions in wheat samples packed in a rectangular plastic container and treated in a 6 kW, 27.12 MHz RF system with and without mixing conditions. The developed model was then experimentally validated by temperature distributions of three layers without mixing condition, and surface and interior temperature distributions of wheat samples under one, two and three times mixing conditions. Both simulation and experiment showed similar heating patterns in RF treated wheat samples under both conditions, in which corners and edges were overheated and the temperatures were higher in the lower sections of the container. The uniformity index (UI) was used to evaluate effects of mixing on RF heating uniformity. Both experimental and simulated UI showed decreasing trend with the increasing mixing times. The developed model can help to understand the RF heating patterns and effects of mixing conditions on RF heating uniformity and provide valuable strategy for developing effective industrial-scale RF treatments with mixing processes.

1. Introduction

Heating with radio frequency (RF) energy has been considered as a novel heating technology for postharvest pasteurization (Gao et al., 2011; Liu et al., 2011; Jeong and Kang, 2014) and disinfestations (Nelson, 1973; Wang and Tang, 2001; Ikediala et al., 2002; Lagunas-Solar et al., 2007; Shrestha and Baik, 2013). Heating uniformity is a major concern for applying RF heating to industrial applications (Jiao et al., 2014; Huang et al., 2015). Non-uniform heating in treated products results in either survivals of pathogens/insects or degraded quality (Wang et al., 2001a, 2005; Tiwari et al., 2011; Jiao et al., 2012; Kim et al., 2012). The heating uniformity index (UI) has been used to evaluate and compare temperature distributions in RF treated samples (Wang et al., 2005, 2008; Alfaifi et al., 2014; Huang et al., 2015). A number of methods have been reported to improve RF heating uniformity, such as hot air surface heating, sample movement, similar surrounding material assistance and mixing (Wang et al., 2007a,b; Gao et al., 2010; Hou et al., 2014; Jiao et al., 2014). Since mixing is usually used in industrial-scale RF treatments (Wang et al., 2006, 2007a), it is important to clearly determine the effects of mixing on temperature distributions in RF treated products.

Mixing can reduce product temperature variations during RF heating as it eliminates the position effect in a container caused by non-uniform electrical field in RF units (Wang et al., 2005). Uniform heating has been achieved by implementation of a single mixing for almonds in the middle of RF treatment periods (Gao et al., 2010). Mixing the walnuts twice during 3 min RF heating improves the heating uniformity of final walnut temperatures (Wang et al., 2006). A single mixing for walnuts is made by a riffle-type sample splitter to obtain the required heating uniformity (Wang et al., 2007a). Twice mixings are carried out through the whole RF treatment to get better heating uniformity and acceptable quality of chestnuts (Hou et al., 2014). Although numerous experimental studies prove that mixing can improve heating uniformity of treated products, there is no computer simulation model to systematically study effects and performances of mixing on RF heating uniformity.

To acquire deep insights on the heating uniformity of products subjected to RF treatments, mathematical models and computer simulation are commonly used as valuable tools with time-saving and low costs. To improve RF heating uniformity, several simulation models have been developed for different food materials, such as meat batters (Marra et al., 2007), soybeans (Huang et al., 2015), wheat flour (Tiwari et al., 2011), raisins (Alfaifi et al., 2014) and peanut butter (Jiao et al., 2014). A number of

* Corresponding author at: College of Mechanical and Electronic Engineering, Northwest A&F University, Yangling, Shaanxi 712100, China. Tel.: +86 29 87092319; fax: +86 29 87091737.
E-mail address: shaojinwang@nwsuaf.edu.cn (S. Wang).

http://dx.doi.org/10.1016/j.compag.2015.08.025
0168-1699/

mathematical models have been developed associated with RF heating under mixing conditions. For example, Wang et al. (2005) developed a mathematical model based on normal distributions of walnut temperatures against frequency to study the influence of intermittent stirrings on RF heating uniformity. This model was further applied to predict the suitable operational time–temperature ranges of walnuts, lentil, soybean and wheat as a function of mixing numbers so as to meet the insect control and product quality (Wang et al., 2008). Although the influence of intermittent stirrings on RF heating uniformity is determined, the mathematical model is developed based on normal sample temperature distributions without detailed simulation of heating patterns influenced by stirring. In addition, there are few reports on the finite element simulation of mixing effects on RF heating uniformity.

The objectives of this study were to (1) develop a computer simulation model for wheat samples at a 6 kW, 27.12 MHz RF system using commercial finite element software COMSOL, (2) validate the computer simulation model using the experimental temperature profiles of wheat samples after RF heating without and with mixing, and (3) predict the effects of mixing on RF heating uniformity based on the uniformity index (UI).

2. Material and methods

2.1. Materials and sample preparation

The wheat (*Triticum aestivum*) sample was obtained from a local farmer in Yangling, Shaanxi, China and stored at the constant temperature (25 °C) in a thermostatic and humidity controlled chamber (BSC-150, Shanghai BoXun Industrial & Commerce Co., Ltd., Shanghai, China) before RF treatments. The initial moisture content of wheat was 8.73 ± 0.12% on wet basis (w.b.). The wheat samples were put in a rectangular container (inner dimension $30 \times 22 \times 6\ cm^3$) for RF treatments. The bottom and side walls of the container were made of thin polypropylene mesh with opening of 6.5 mm and thickness of 3 mm. To prevent wheat leakage from the container, the internal surfaces of the container were covered by a thin layer of plastic film with mesh opening of 1 mm.

2.2. Development of computer model

2.2.1. Physical model

A 6 kW, 27.12 MHz free-running oscillator RF system with parallel-plate electrodes (COMBI 6-S, Strayfield International Limited, Wokingham, UK) was used for RF treatments. The RF system consisted of metallic enclosure, generator, and RF applicator with top and bottom electrodes (Fig. 1). The bottom electrode was integrated into metallic enclosure. The electrode gap was changed by adjusting position of the top electrode to achieve the required RF power. The sample was placed on the bottom electrode and sandwiched between top and bottom electrodes. The dielectric material was heated up because of converting electromagnetic energy into thermal energy.

2.2.2. Governing equations

The Maxwell's equations can be solved to obtain the electric field intensity in the electromagnetic field. Since the wavelength (11 m) in the 27.12 MHz RF system is often much larger than the electrode gap so that the Maxwell's equation can be simplified to the Laplace equation with a quasi-static assumption (Metaxas, 1996):

$$-\nabla \cdot ((\sigma + j2\pi f \varepsilon_0 \varepsilon')\nabla V) = 0 \quad (1)$$

The Laplace equation was solved in both treated sample and surrounding air, so σ is the electrical conductivity of the heated sample or air (S m^{-1}) and ε' is also the dielectric constant of food material or air, depending on which domain the equation is solved. $j = \sqrt{-1}$, f is the frequency (Hz), ε_0 is the permittivity of free space (8.86×10^{-12} F m^{-1}) and V is the voltage between the two electrodes (V).

The heat conduction equation was just solved within the food material, convection at the sample's surface and heat generation in the food due to RF energy. The heat transfer inside the treated sample is described by Fourier's equation (Uyar et al., 2015):

$$\rho C_p \frac{\partial T}{\partial t} = \nabla \cdot (k \nabla T) + Q \quad (2)$$

where $\partial T/\partial t$ is the heating rate in food samples (°C s^{-1}), k is the thermal conductivity (W m^{-1} K^{-1}), ρ and C_p are the density (kg m^{-3}) and specific heat (J kg^{-1} K^{-1}), respectively. Q is the RF power conversion to thermal energy (W m^{-3}) within the food sample under an electric field intensity ($|\vec{E}|$, V m^{-1}) and described as (Choi and Konrad, 1991):

$$Q = 2\pi f \varepsilon_0 \varepsilon'' \left|\vec{E}\right|^2 \quad (3)$$

where the electric field intensity is $\vec{E} = -\nabla V$, ε'' is the loss factor of the food sample.

2.2.3. Initial and boundary conditions

The geometrical, thermal and electrical boundary conditions of the RF system used in the simulation are presented in Fig. 1. The initial temperature was set at 25 °C. Except for the top surface was uncovered and exposed to the ambient air, the side walls and bottom of the sample were surrounded by a rectangular plastic container (Fig. 1a). The top exposed surface of the sample was assigned with convective heat transfer (h = 20 W m^{-2} K^{-1}) for free convection of ambient air (Wang et al., 2001b). The top electrode was set as the electromagnetic source since it introduced high frequency electromagnetic energy from the generator to the heating cavity and the bottom electrode was set as ground (V = 0 V). It was difficult to measure the actual top electrode voltage during operating without disturbing the electric field (Marshall and Metaxas, 1998), therefore, preliminary simulations with the same conditions were run by considering different values for the voltage of top electrode. Based on the comparison between preliminary simulated and experimental results, the top electrode voltage was considered as 15,000 V (amplitude of the sinusoidal voltage) for the final simulation. The same approach has been used to evaluate top electrode voltage of similar RF systems (Marshall and Metaxas, 1998; Birla et al., 2008; Tiwari et al., 2011; Alfaifi et al., 2014). All the metal shielding parts except for the top electrode were grounded, and considered as electrical insulation ($\nabla \cdot E = 0$).

2.2.4. Model development under mixing conditions

2.2.4.1. Model assumptions. To simulate temperature distributions of wheat sample subjected to RF heating under mixing conditions, the following assumptions were considered:

(1) After each mixing, the temperature distributions of wheat sample were assumed to be uniform, because of small standard deviations after short RF heating at each mixing step.
(2) The mass and momentum transfers of moisture were neglected due to a short time (3.5 min) RF heating.

2.2.4.2. Model descriptions. Once, twice and thrice mixings were performed outside the RF cavity by hands in a large container at predetermined intervals during the whole treated time (3.5 min). In the simulation model, after one-time mixing for one interval

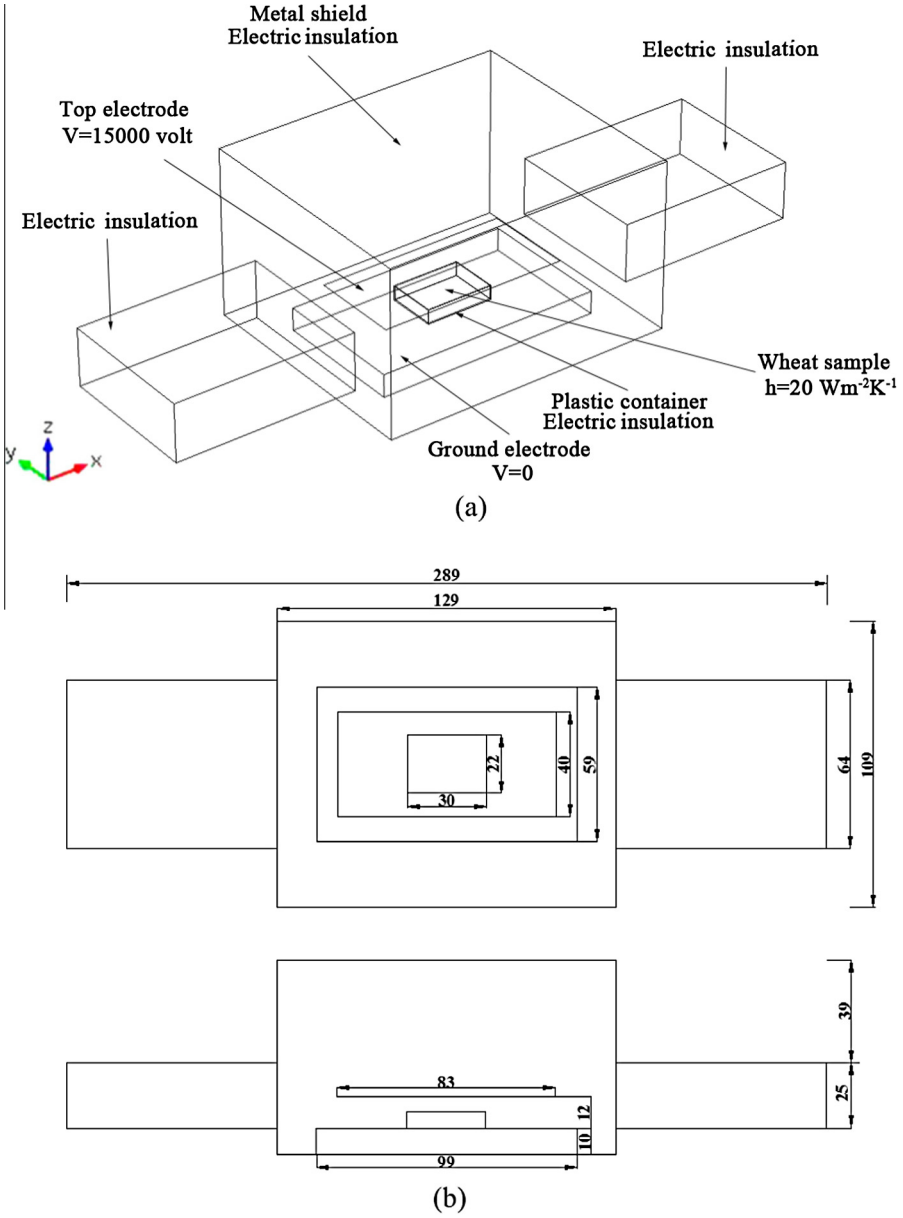

Fig. 1. 3-D scheme (a) and dimensions (b) of the 6 kW 27.12 MHz RF system and food load (wheat sample) used in simulations (all dimensions are in cm).

RF heating, the average temperature of wheat samples was regarded as the initial temperature for the next interval RF heating until all mixing times were completed. The temperature drop (ΔT, °C) due to heat loss during each mixing process was considered in simulation model as follows:

$$\Delta T = \frac{hA(T_f - T_a)\Delta t}{\rho C_p V} \quad (4)$$

where h, the convective heat coefficient which was estimated to be 28 W m^{-2} K^{-1} with forced convection during the whole mixing process (Wang et al., 2007a), A and V are the whole surface areas (0.1944 m^2) and volume (0.00396 m^3) of the wheat sample, respectively. T_f and T_a are the final average temperature of wheat sample after RF heating prior to each mixing and the ambient air temperature (25 °C), respectively. Δt is the total time (60 s) taken during each mixing process.

2.2.5. Simulation procedure

Commercial software COMSOL Multiphysics based on finite element method (FEM) (V4.3a COMSOL Multiphysics, CnTech Co., Ltd., Wuhan, China) was used to simulate the RF heating process. The Joule heating module used in this study was a combination module of electromagnetic heating and heat transfer, which can solve the electromagnetic equations and heat transfer equations simultaneously. The software was run on Hewlett–Packard workstation with a Core (TM) i5-2400, 3.10 GHz Intel Core Processor and 8 GB RAM operating with Windows 7 64-bite operating system. Extremely fine mesh was created near the sharp edges and corners of the wheat sample and container to improve the accuracy of the results. The mesh size was determined based on the convergence study when the temperature difference between successive calculations was less than 0.1%. The final mesh system consisted of 319,153 domain elements (tetrahedral), 39,234 boundary elements (triangular), 1414 edge elements (linear) and 57 vertex elements, was used in subsequent simulation runs. The maximum and minimum

Table 1
Electrical and thermo-physical properties of bulk materials used in computer simulation (adapted from Chen et al. (2015)).

Material properties	Wheat	Aluminum[a]	Air[a]	Polypropylene[a]
Heat capacity C_p (J kg^{-1} K^{-1})	2670[d]	900	1200	1800
Density ρ(kg m^{-3})	860	2700	1.2	900
Thermal conductivity k (W m^{-1} K^{-1})	0.15[c]	160	0.025	0.2
Dielectric constant (ε')	4.30[d]	1	1	2.0[b]
Loss factor (ε'')	0.11[d]	0	0	0.0023[b]

Source:
[a] COMSOL material library, V4.3a (2012).
[b] von Hippel (1995).
[c] Li et al. (2010).
[d] Shrestha and Baik (2013).

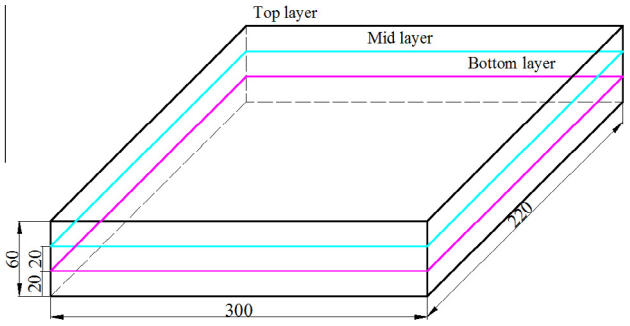

Fig. 2. Dimensions of the plastic container and three layers for surface temperature measurements in experiments without mixing (all dimensions are in mm).

mesh element sizes were 0.159 m and 0.007 m, respectively. Time step was determined by the max iteration per time step. If the computations were convergent before the max iteration, the time step could be short and it would start next iteration automatically. Generally, to guarantee the convergence of computation, the initial time step was set at a short one and changed during processing. In this study, the max iteration per time step was 10,000. Initial and maximum time steps were set as 0.001 and 1 s. Each computation case took about 25 min to complete.

2.2.6. Model parameters

Information of dielectric, thermal, and physical properties of the treated products and surrounding medium is essential in modeling the RF heating process. Table 1 lists these values of bulk wheat, polypropylene, aluminum and air in the computer model. Although

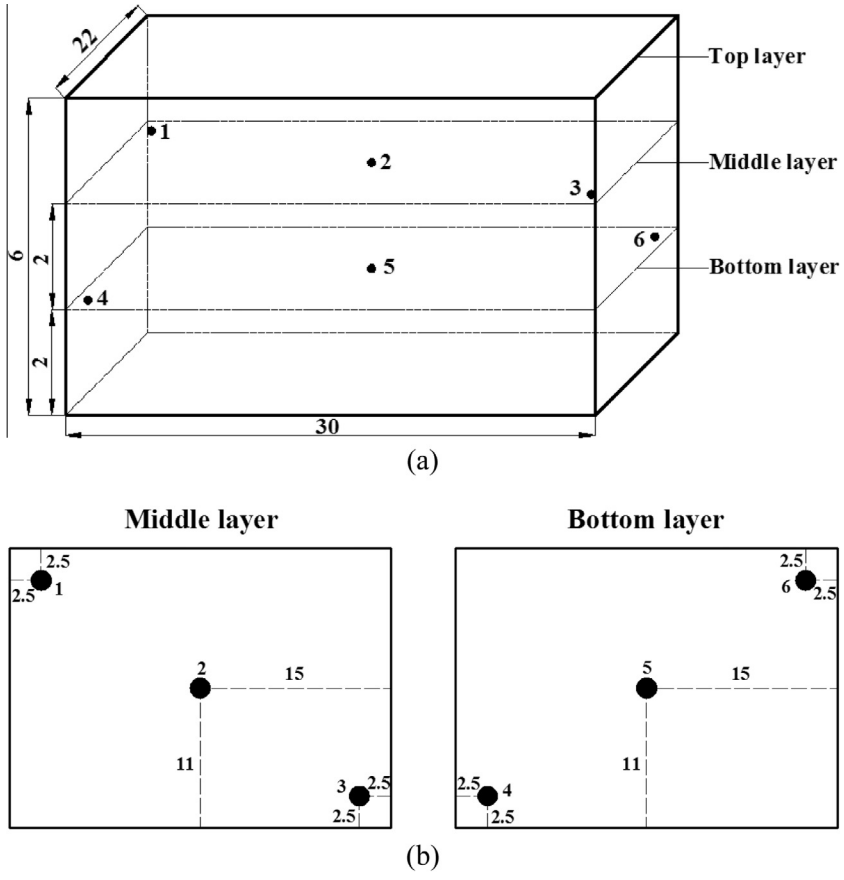

Fig. 3. Top layer (a) and the locations of six points (b) in wheat samples used for surface and interior temperature measurements in mixing experiments (all dimensions are in cm).

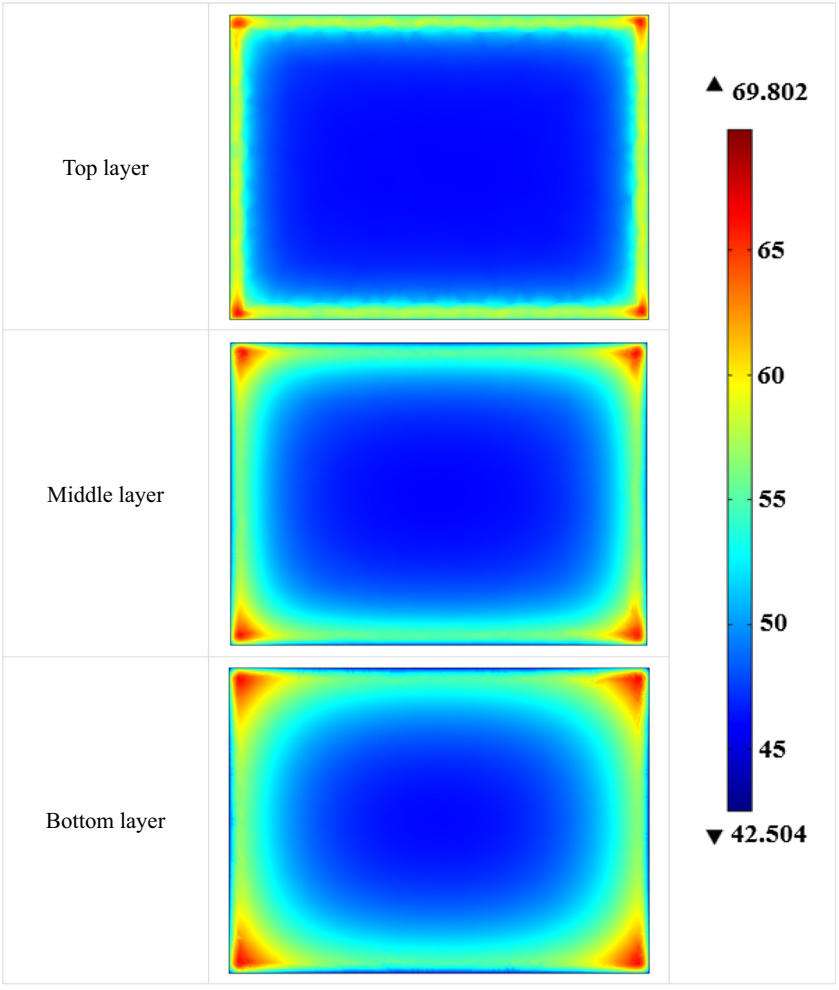

Fig. 4. Simulated temperature profiles (°C) of wheat samples (300 × 220 × 60 mm^3) at (a) three horizontal layers (20, 40, and 60 mm) and (b) three vertical layers (50, 150, and 250 mm), after 3.5 min RF heating without mixing at an electrode gap of 120 mm and initial temperature of 25 °C.

dielectric and thermal properties of bulk wheat samples are dependent on temperature and moisture content, they changed slightly with a limited temperature range (25–60 °C) and moisture content of 8.7% w.b. The average values of bulk wheat properties over the tested temperature and moisture ranges obtained from the literature (Li et al., 2010; Shrestha and Baik, 2013) are also listed in

Table 1. The same method with constant dielectric and thermal properties has been used in simulations of peanut butter and soybeans (Jiao et al., 2014; Huang et al., 2015).

2.3. Model validation

2.3.1. Experiment without mixing

The RF heating unit was used in experiments to validate the computer simulation model. About 3.39 kg wheat with bulk density of 860 kg m^{-3} was put into the rectangular container and placed at the center of the ground electrode in the RF cavity. Two very thin polypropylene films were used to separate the container into three layers with each filled with 1.13 kg wheat (Fig. 2), which are convenient to map the surface temperature distributions in three layers (top, middle, and bottom) using thermal imaging cameras after RF heating. Prior to the RF treatment, the wheat was equilibrated at room temperature at 25 °C for 12 h. The lethal temperature range for the complete mortality of many insects including *Cryptolestes Ferrungineus S.* at all life stages are within 45–60 °C (Johnson et al., 2004; Shrestha et al., 2013) with different holding time. To meet the required mortality of the target insects and acceptable quality of agricultural products, the wheat sample was subjected to RF heating without mixing for 3.5 min with 120 mm electrode gap until the central sample temperature reached 45 °C, which was monitored and recorded by a fiber optic sensor system (HQ-FTS-D120, Xi'an HeQi Opo-electronic Technology Co., Ltd., Shaanxi, China) with an accuracy of ±1 °C. After the RF unit was turned off, the container was immediately taken out of the RF system for the surface temperature mapping of all three layers of wheat starting from top to bottom layer by an infrared camera (DM63-S, DaLi Science and Technology Co., Ltd., Zhejiang China) with an accuracy of ±2 °C. Details on the measurement procedure can be found in Wang et al. (2007a). All the three thermal imaging recordings were completed in 30 s. The image analysis system (V1.0, DaLi Science and Technology Co., Ltd., Zhejiang, China) was used to collect and analyze the surface temperature data points for each layer. The experiments were replicated two times. Experimental and simulated temperature profiles of wheat were compared both in the container center and at three layers.

2.3.2. Mixing experiments

The same wheat sample was used for mixing experiments with an electrode gap of 120 mm during the whole 3.5 min RF heating. The experiments were carried out at intervals of 105 s for one mixing treatment experiment, 70 s for two mixing treatments experiment and 52.5 s for three mixing treatments experiment, respectively, during the entire treatment time. Mixing was conducted manually outside the RF cavity in a larger container

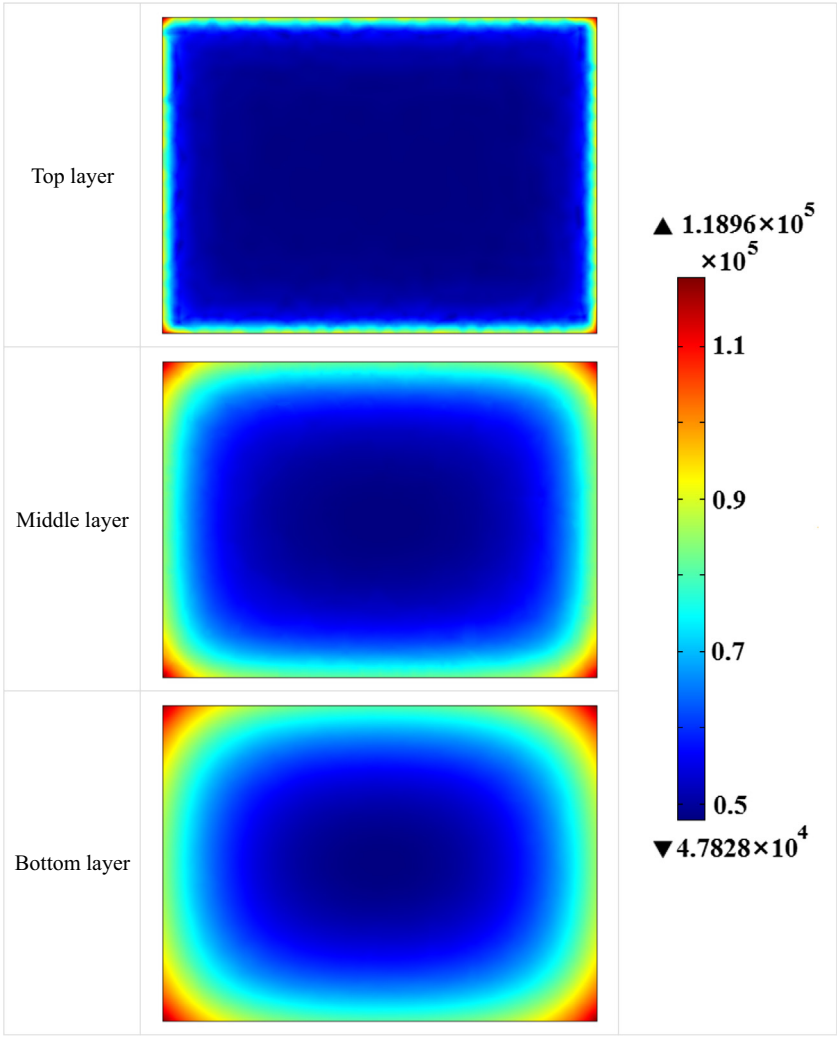

Fig. 5. Simulated E-field distributions (V/m) of wheat samples (300 × 220 × 60 mm^3) at three horizontal layers (20, 40, and 60 mm) after 3.5 min RF heating without mixing at an electrode gap of 120 mm and initial temperature of 25 °C.

($35.5 \times 27.5 \times 10.5\ cm^3$) for 25 s, and then the samples were returned to the treatment container and put back into the RF system for further heating under the same conditions. After the predetermined mixing times were completed, samples were placed back into the RF cavity for the remainder of the heating time. Each whole mixing process took about 60 s. Before and immediately after RF treatments, surface temperatures of the top layer of wheat samples in the container were measured with the same infrared camera described above. Each measurement took about 3 s. The surface temperature data of the top layer were used to calculate the average and standard deviation values. Six points (Fig. 3) were selected in the middle and bottom layers of wheat samples for interior temperature measurements before and after mixing treatments using a thin Type-T thermocouple thermometer (TMQSS-020-6, Omega Engineering Ltd., CT, USA). Each test was repeated twice.

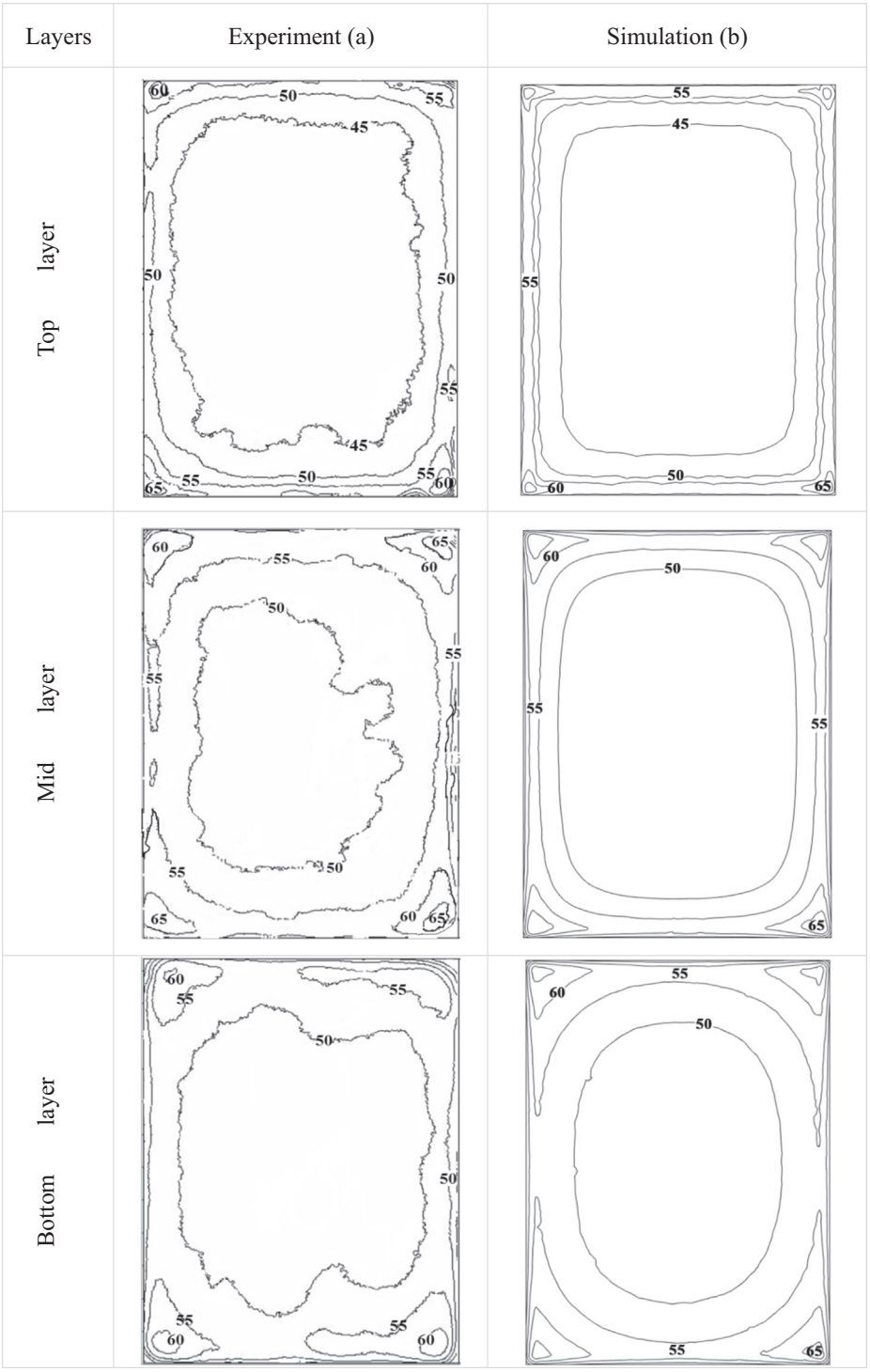

Fig. 6. Experimental and simulated temperature distributions (°C) of wheat samples at top, middle, and bottom layers (20, 40, and 60 mm from the bottom of sample) in a plastic container ($300 \times 220 \times 60\ mm^3$) on the center of the ground electrode, after 3.5 min RF heating without mixing at an initial temperature of 25 °C and a fixed electrode gap of 120 mm.

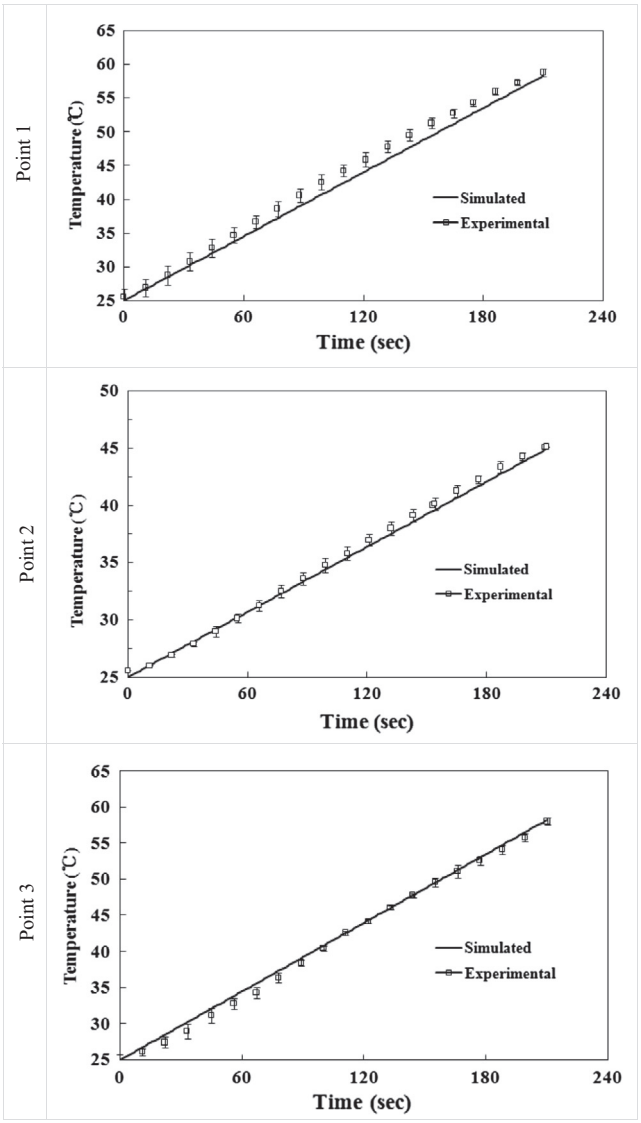

Fig. 7. Experimental and simulated temperature–time histories of wheat samples at three points of second mid layer (Fig. 3) from the bottom of sample ($300 \times 220 \times 60$ mm^3), placed in a rectangular container on the center of the bottom electrode during 3.5 min RF heating without mixing at an electrode gap of 120 mm.

2.4. Heating uniformity evaluation

Heating uniformity index (λ) was used to evaluate the effects of mixing on wheat samples. The λ value has been used to evaluate the temperature uniformity of samples subjected to RF heating (Gao et al., 2010; Jiao et al., 2012), which is defined as the ratio of standard deviation to average temperature rise during heating, using the following equation (Wang et al., 2008):

$$\lambda = \frac{\sqrt{\sigma^2 - \sigma_0^2}}{\mu - \mu_0} \quad (5)$$

where μ and μ_0 are final and initial mean wheat temperatures (°C), and σ and σ_0 are final and initial standard deviation (°C) of wheat temperatures over treatment time, respectively.

3. Results and discussion

3.1. Simulated temperature profiles for wheat sample

Fig. 4 shows the simulated temperature profiles of RF treated (without mixing) wheat in three horizontal (20, 40, and 60 mm) and three vertical (50, 150, and 250 mm) layers with an initial temperature of 25 °C after 3.5 min RF heating at a fixed electrode gap of 120 mm. In the horizontal layers, the sample temperatures were higher in the middle and the bottom layers (44.0–70.9 °C and 45.1–69.3 °C), but lowest in the top layer (42.5–68.3 °C). The average temperatures of middle layer and bottom layer of wheat were higher, which might be caused by more RF energy absorbed in these layers due to concentrated electric field in lower sections (near the bottom electrode) of wheat samples (Fig. 5). Fig. 5 presents electric field distributions of three horizontal layers of the wheat sample and shows that the electric field intensities in middle and bottom layers were stronger than those in the top one. The simulated RF heating of model fruit, placed on the bottom electrode also showed higher heating rate at the lower part of the fruit (Birla et al., 2008). Similar RF heating patterns were reported in wheat flour (Tiwari et al., 2011), and soybeans (Zhu et al., 2014; Huang et al., 2015). The lowest temperature of top layer could be resulted from the heat loss and the evaporative cooling effect on the outer surface of the wheat. In the vertical layers, the sample temperature increased from the middle section to the outer section, whereas was lower at the interface of side walls of the polypropylene container. The highest temperature values were observed at the edges and corners of all the three layers (Fig. 4a), which could be due to the deflected electric field at those sections (Barber, 1983). The edges and corners of all three layers had stronger electric field intensities than the middle sections of wheat samples (Fig. 5). Since the RF power density at any sample location is proportional to the square of electric field, higher temperature values were observed at these parts (Huang et al., 2015). Similar heating results have been observed for walnuts (Wang et al., 2007a,b), raisins (Alfaifi et al., 2014) and peanut butter (Jiao et al., 2014).

3.2. Model validation without mixing conditions

The surface temperature contours of the wheat samples obtained from experiments and simulation for the three horizontal layers (top, middle, and bottom) after 3.5 min RF treatment without mixing at a fixed electrode gap are presented in Fig. 6. Temperature distribution comparisons indicated a good agreement

Table 2
Comparison between experimental and simulated average and standard deviation temperatures (°C) of wheat samples at three horizontal layers after 3.5 min RF heating without mixing at a fixed gap of 120 mm and initial temperature of 25 °C.

Layer	Experiment	Simulation
Top	48.7 ± 4.1	48.9 ± 5.5
Middle	51.2 ± 3.2	52.4 ± 5.5
Bottom	52.0 ± 2.2	52.4 ± 5.1

Table 3
Comparison of temperature distribution (Average ± SD) of wheat samples between experiment and simulation subjected to 3.5 min RF heating before and after mixing at a fixed gap of 120 mm.

Temperatures (°C)		Mixing		
		1st	2nd	3rd
Experiment (surface)	Before mixing	31.3 ± 1.0	37.1 ± 0.8	42.4 ± 0.8
	After mixing	31.1 ± 0.5	36.7 ± 0.6	41.8 ± 0.6
Experiment (internal)	Before mixing	32.3 ± 1.9	38.4 ± 1.8	43.8 ± 1.5
	After mixing	31.5 ± 0.7	37.4 ± 0.3	42.8 ± 0.4
Simulation	Before mixing	31.4 ± 1.4	37.4 ± 1.4	43.3 ± 1.4
	After mixing	31.2 ± 0.0	37.0 ± 0.0	42.6 ± 0.0

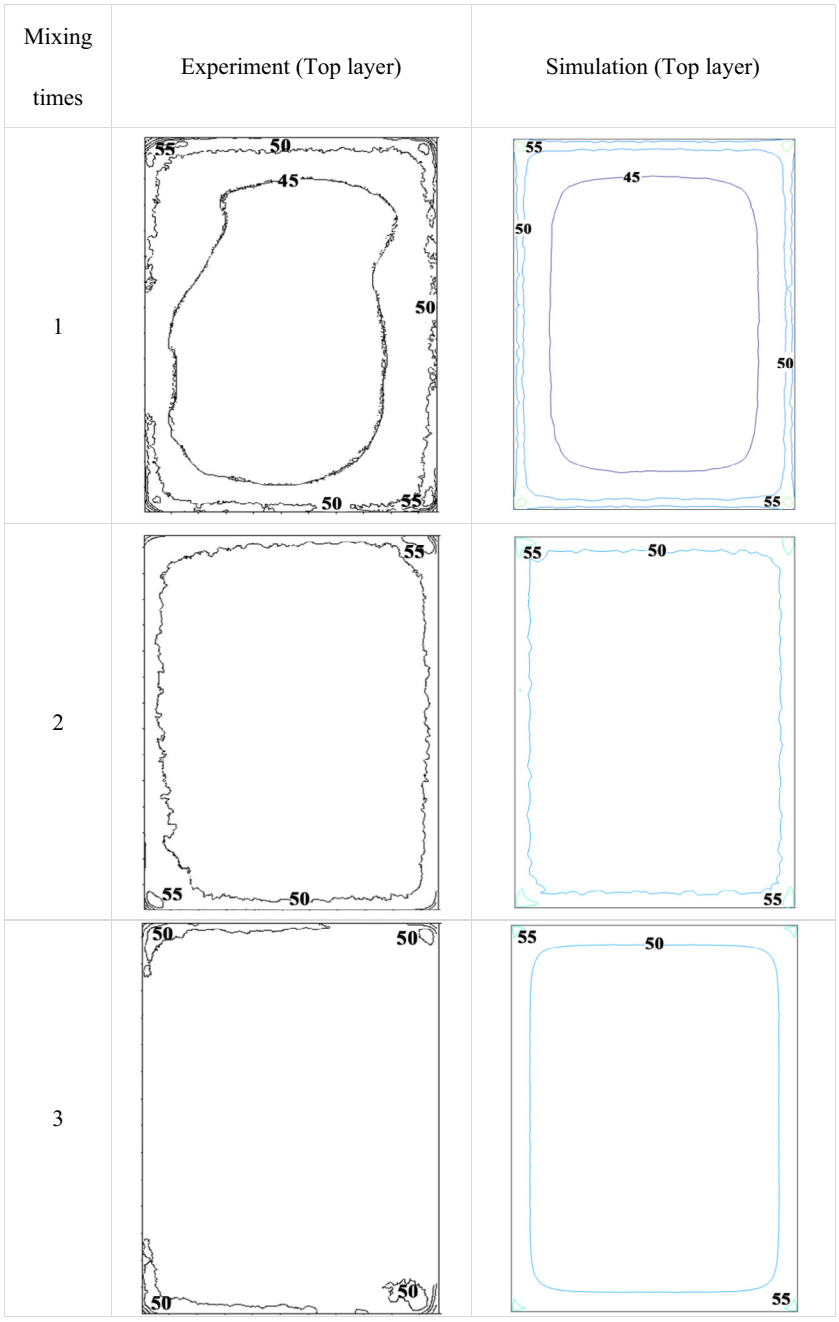

Fig. 8. Experimental and simulated surface temperature distributions (°C) of wheat samples at the top layer (60 mm from the bottom of sample) in a plastic container ($300 \times 220 \times 60$ mm^3) corresponded to one, two and three-time mixings during 3.5 min RF heating at an initial temperature of 25 °C and a fixed electrode gap of 120 mm.

between experimental and simulated three layers. Both experiment and simulation showed hot spots at corners and edges of the top, middle and bottom layers but cold ones in the central section. The maximum temperature differences between experiment and simulation were found to be about 2, 3, and 5 °C at corners and edges in top, middle, and bottom layers, respectively. The difference might be caused by the simplification of the RF unit or neglected water and heat loss in the possible evaporation of the wheat sample in the simulation model.

The experimental temperature profile at the three points of middle layer (Fig. 3) also showed good agreements with the simulated one (Fig. 7). Table 2 compared the experimental and simulated mean and standard deviation temperatures of wheat samples in all three horizontal layers after 3.5 min RF heating without mixing at a fixed gap of 120 mm. Less than 1 °C was obtained between experimental and simulated average temperatures in all three layers, suggesting an acceptable model precision.

Table 4
Comparison between experimental and simulated surface temperatures of wheat samples at the top layer after 0, 1, 2 and 3 times mixing during 3.5 min RF heating with an initial temperature of 25 °C and a fixed electrode gap of 120 mm.

Mixing times	Experiment (top layers)	Simulation (top layers)
0	48.7 ± 4.1	48.9 ± 5.5
1	47.5 ± 1.6	48.6 ± 3.2
2	47.3 ± 1.1	48.3 ± 2.3
3	47.0 ± 0.9	47.9 ± 1.8

Table 5
Experimental and simulated wheat temperatures at interior six locations as influenced by mixing times during 3.5 min RF heating with an initial temperature of 25 °C and a fixed electrode gap of 120 mm.

Mixing times	Locations	Experimental temp (°C)	Simulated temp (°C)
0	1	55.5 ± 0.08	59.5
	2	46.0 ± 0.21	46.5
	3	56.7 ± 0.14	59.6
	4	55.0 ± 0.28	60.9
	5	47.0 ± 0.22	47.0
	6	53.9 ± 0.15	60.9
1	1	53.1 ± 0.07	54.5
	2	46.6 ± 0.06	47.2
	3	53.7 ± 0.07	54.6
	4	53.6 ± 0.11	55.3
	5	47.7 ± 0.22	47.7
	6	52.4 ± 0.57	55.4
2	1	52.4 ± 0.35	52.6
	2	47.4 ± 0.42	48.1
	3	53.0 ± 0.30	52.8
	4	51.5 ± 0.71	53.2
	5	48.3 ± 0.35	48.4
	6	51.6 ± 0.50	53.3
3	1	50.0 ± 0.57	51.6
	2	49.3 ± 0.06	49.1
	3	51.1 ± 0.43	51.6
	4	50.0 ± 0.57	52.2
	5	48.9 ± 0.11	49.2
	6	49.9 ± 0.15	52.1

However, the simulated standard deviations were comparatively higher than those determined by experiments, which may be due to the finer mesh of corners and edges than those in central parts of wheat samples in the model while those are distributed equally in the experiment.

3.3. Model validation under mixing conditions

Table 3 shows comparison of surface temperature distribution of wheat samples between experiment and simulation subjected to 3.5 min RF heating before and after mixing. The temperature drop was small after each mixing both based on the experimental and simulation results, suggesting that the heat loss during short mixing was small and the given convective heat transfer coefficient was reasonable for Eq. (4). The standard deviation of sample temperatures was clearly reduced after short mixing due to thorough and random changes of the sample particle positions. Especially for only one-time mixing during whole process, the standard deviation was reduced from 2.6 to 0.4 °C, which could be close to the assumption for mixing conditions in the simulation model.

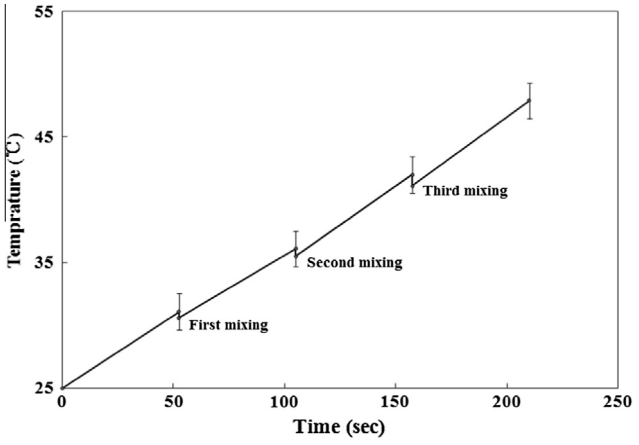

Fig. 9. Change of simulated average and standard deviation temperatures of wheat sample during three-time mixing process for 52.5 s of each RF heating interval.

Fig. 8 shows the experimental and simulated surface temperature distributions of the wheat samples in three top layers after one, two and three-time mixings during 3.5 min RF heating at a fixed gap of 12 cm. In general, the experimental surface temperatures in three top layers under mixing conditions showed a good agreement with the simulated results. The average and standard deviation temperatures of wheat samples were compared between the simulation and experiment in the top layer corresponded to 0, 1, 2 and 3-time mixings during 3.5 min RF heating (Table 4). The maximum temperatures of top layers were 66.5 °C, 60.6 °C, 56.9 °C and 51.0 °C in experiment and 68.3 °C, 61.7 °C, 58.4 °C and 55.3 °C in simulation, respectively, after 0, 1, 2 and 3-time mixings during the whole treatment time. The maximum temperature differences in the top layer between experiment and simulation were about 2, 1, 2 and 4 °C for 0, 1, 2 and 3-time mixings, respectively. Table 5 summarizes the interior temperature values of wheat samples at six points in experiment and simulation (Fig. 3). With increasing mixing times from 0 to 3 times, the temperatures of central points (2 and 5) at mid and bottom layers increased gradually, whereas the temperatures of corner and edge points (1, 3, 4 and 6) of these two layers decreased both in experiments and simulations. During the mixing process, the positions of wheat were randomly changed and redistributed evenly through the sample (Wang et al., 2005, 2007a), resulting in good mixing of wheat at top and bottom layers or at hot spots of corners and edges and cold spots at central sections. After mixing, the temperature variations between central parts and corner and edge parts were reduced and uniform heating of wheat samples could be obtained.

Fig. 9 presents the change of average and standard deviation temperatures during three-time mixing for 52.5 s of each RF heating interval in simulation. The wheat temperature increased generally with increasing RF heating time. After mixing each step, the temperature distribution of wheat sample was uniform, but a slight reduction of average temperature was obtained due to heat loss, which is similar to that reported for RF treated walnuts with mixing (Wang et al., 2006).

3.4. Heating uniformity evaluation

Before RF treatment, the initial temperature of wheat samples was 25 ± 0.20 °C. Table 6 lists the temperature distributions and values of uniformity index (UI) of the top layer (surface temperature) and the interior wheat samples (interior temperatures at 6 locations) in the plastic container without and with mixing conditions in experiment and computer simulation. Both the average temperatures of surface and interior wheat samples were reduced in experiment and simulation under mixing conditions, and this

Table 6
Comparison of surface and interior temperature distribution (average ± SD) and heating uniformity index (UI) of surface and interior wheat samples subjected to 3.5 min RF heating without and with mixing conditions at a fixed gap of 120 mm.

Temperature distribution and UI	Mixing times			
	0	1	2	3
Experiment				
Surface temperature (°C)	48.7 ± 4.1	47.5 ± 1.6	47.3 ± 1.1	47.0 ± 0.9
Interior temperature (°C)	52.3 ± 4.5	51.1 ± 3.0	50.7 ± 2.2	49.8 ± 0.7
Surface heating UI	0.1738	0.0691	0.0503	0.0403
Interior heating UI	0.1626	0.1157	0.0850	0.0279
Simulation				
Surface temperature (°C)	48.9 ± 5.5	48.6 ± 3.2	48.3 ± 2.3	47.9 ± 1.8
Interior temperature (°C)	55.7 ± 7.00	52.5 ± 3.9	51.4 ± 2.5	51.0 ± 1.4
Surface heating UI	0.2302	0.1335	0.0978	0.0787
Interior heating UI	0.2275	0.1417	0.0932	0.0551
Volume heating UI	0.1960	0.1075	0.0764	0.0603

slight reduction in the mean temperature was probably caused by heat losses from the wheat samples to the surrounding environment during mixing. The standard deviation of sample temperatures decreased with increasing mixing number. The same phenomenon was found at mixing walnuts (Wang et al., 2005, 2008), chestnuts (Hou et al., 2014), and almonds (Gao et al., 2010). In practical applications using several RF systems in series with mixings in between, forced hot air should be used to minimize the amount of heat loss during the mixing process (Wang et al., 2005). In addition, the wheat sample with relative low temperature at the top sections could also be increased by using additional surface hot air heating and placing the sample in the middle of two electrodes. The uniformity index (UI) showed the same decreasing trend with increasing mixing times both in experiment and simulation (Table 6), resulting in the improved heating uniformity of RF treated wheat samples. Simulated UI values were similar for surface, interior and volume samples, suggesting negligible influence of mesh element size on UI estimation. The same results have also been reported for stirring and mixing walnuts, soybean, lentil, wheat, and chestnut (Wang et al., 2007a,b, 2008; Hou et al., 2014).

4. Conclusions

A computer model was developed to simulate wheat sample with and without mixing conditions subjected to RF heating in a 6 kW, 27.12 MHz RF system. Results both from computer simulation and experiment showed good agreements for the temperature distributions of wheat samples under 0, 1, 2 and 3-time mixing conditions. Under mixing conditions, the maximum temperature of top layer in wheat sample reduced from 66.5 °C to 51.0 °C in experiment and from 68.3 °C to 56.1 °C in simulation after three-time mixing during 3.5 min RF heating. Because of the heat loss during mixing process, both the average temperatures of surface and interior wheat samples were also reduced in experiment and simulation. The uniformity index (UI) of RF treated wheat samples showed the same decreasing trend with the increasing mixing times based on experiment and simulation results. The RF heating uniformity was improved by mixing based on the reduced UI. This validated model can be used to understand the RF heating patterns and effects of mixing conditions on RF heating uniformity. Furthermore, the model can serve as a valuable tool to design and optimize a treatment protocol for industrial-scale RF treatments.

Acknowledgements

This research was conducted in the College of Mechanical and Electronic Engineering, Northwest A&F University, and supported by research grants from Ph.D. Programs Foundation of Ministry of Education of China (20120204110022) and General Program of National Natural Science Foundation in China (31371853). We thank all members of agricultural product processing lab for their helps.

References

Alfaifi, B., Tang, J., Jiao, Y., Wang, S., Rasco, B., Jiao, S., Sablani, S., 2014. Radio frequency disinfestation treatments for dried fruit: model development and validation. J. Food Eng. 120, 268–276.
Barber, H., 1983. Electroheat, first ed. Granada Publishing Limited, London, UK.
Birla, S.L., Wang, S., Tang, J., 2008. Computer simulation of radio frequency heating of model fruit immersed in water. J. Food Eng. 84 (2), 270–280.
COMSOL Material Library. 2012. COMSOL Multiphysics, V4.3a, Burlington, MA, USA.
Choi, C., Konrad, A., 1991. Finite element modeling of the RF heating process. IEEE Trans. Magn. 27 (5), 4227–4230.
Chen, L., Huang, Z., Wang, K., Li, W., Wang, S., 2015. Simulation and validation of radio frequency heating with conveyor movement. J. Electromagnet. Waves Appl., in review
Gao, M., Tang, J., Villa-Rojas, R., Wang, Y., Wang, S., 2011. Pasteurization process development for controlling Salmonella in in-shell almonds using radio frequency energy. J. Food Eng. 104 (2), 299–306.
Gao, M., Tang, J., Wang, Y., Powers, J., Wang, S., 2010. Almond quality as influenced by radio frequency heat treatments for disinfestation. Postharvest Biol. Technol. 58 (3), 225–231.
Hou, L., Ling, B., Wang, S., 2014. Development of thermal treatment protocol for disinfesting chestnuts using radio frequency energy. Postharvest Biol. Technol. 98, 65–71.
Huang, Z., Zhu, H., Yan, R., Wang, S., 2015. Simulation and prediction of radio frequency heating in dry soybeans. Biosyst. Eng. 129, 34–47.
Ikediala, J., Hansen, J., Tang, J., Drake, S., Wang, S., 2002. Development of a saline water immersion technique with RF energy as a postharvest treatment against codling moth in cherries. Postharvest Biol. Technol. 24 (2), 209–221.
Jeong, S.G., Kang, D.H., 2014. Influence of moisture content on inactivation of *Escherichia coli* O157:H7 and *Salmonella* enterica serovar Typhimurium in powdered red and black pepper spices by radio-frequency heating. Int. J. Food Microbiol. 176, 15–22.
Jiao, S., Johnson, J.A., Tang, J., Wang, S., 2012. Industrial-scale radio frequency treatments for insect control in lentils. J. Stored Prod. Res. 48, 143–148.
Jiao, Y., Tang, J., Wang, S., 2014. A new strategy to improve heating uniformity of low moisture foods in radio frequency treatment for pathogen control. J. Food Eng. 141, 128–138.
Johnson, J., Valero, K., Wang, S., Tang, J., 2004. Thermal death kinetics of red flour beetle (Coleoptera: Tenebrionidae). J. Econ. Entomol. 97 (6), 1868–1873.
Kim, S.Y., Sagong, H.G., Choi, S.H., Ryu, S., Kang, D.H., 2012. Radio-frequency heating to inactivate Salmonella Typhimurium and *Escherichia coli* O157:H7 on black and red pepper spice. Int. J. Food Microbiol. 153 (1–2), 171–175.
Lagunas-Solar, M., Pan, Z., Zeng, N., Truong, T., Khir, R., Amaratunga, K., 2007. Application of radio frequency power for non-chemical disinfestation of rough rice with full retention of quality attributes. Appl. Eng. Agric. 23 (5), 647–654.
Li, Y., Zhang, L., Cao, Y., Zhu, Q., Feng, J., Shen, G., 2010. Determination of thermal conductivity of wheat. Henan Univ. Technol.: Nat. Sci. 31 (1), 67–70.
Liu, Y., Tang, J., Mao, Z., Mah, J.-H., Jiao, S., Wang, S., 2011. Quality and mold control of enriched white bread by combined radio frequency and hot air treatment. J. Food Eng. 104 (4), 492–498.
Marra, F., Lyng, J., Romano, V., McKenna, B., 2007. Radio-frequency heating of foodstuff: solution and validation of a mathematical model. J. Food Eng. 79 (3), 998–1006.
Marshall, M.G., Metaxas, A.C., 1998. Modeling of the radio frequency electric field strength developed during the RF assisted heat pump drying of particulates. J. Microw. Power Electromagn. Energy. 33 (3), 167–177.
Metaxas, A., 1996. Foundations of Electroheat: A Unified Approach Fuel and Energy Abstracts. Elsevier Science.
Nelson, S.O., 1973. Insect-control studies with microwaves and other radio frequency energy. Bull. ESA 19 (3), 157–163.
Shrestha, B., Baik, O.-D., 2013. Radio frequency selective heating of stored-grain insects at 27.12 MHz: a feasibility study. Biosyst. Eng. 114 (3), 195–204.
Shrestha, B., Yu, D., Baik, O.-D., 2013. Elimination of *Cruptolestes Ferrungineus S.* in wheat by radio frequency dielectric heating at different moisture contents. Prog. Electromagn. Res. 139, 517–538.
Tiwari, G., Wang, S., Tang, J., Birla, S.L., 2011. Computer simulation model development and validation for radio frequency (RF) heating of dry food materials. J. Food Eng. 105 (1), 48–55.
Uyar, R., Bedane, T.F., Erdogdu, F., Koray Palazoglu, T., Farag, K.W., Marra, F., 2015. Radio-frequency thawing of food products – a computational study. J. Food Eng. 146, 163–171.
von Hippel, A.R., 1995. Dielectric Materials and Applications. Arctech House, Boston, USA.
Wang, S., Tang, J., 2001. Radio frequency and microwave alternative treatments for insect control in nuts: a review. Agric. Eng. J. 10 (3&4), 105–120.
Wang, S., Ikediala, J., Tang, J., Hansen, J., Mitcham, E., Mao, R., Swanson, B., 2001a. Radio frequency treatments to control codling moth in in-shell walnuts. Postharvest Biol. Technol. 22 (1), 29–38.
Wang, S., Tang, J., Cavalieri, R., 2001b. Modeling fruit internal heating rates for hot air and hot water treatments. Postharvest Biol. Technol. 22 (3), 257–270.
Wang, S., Monzon, M., Johnson, J.A., Mitcham, E.J., Tang, J., 2007a. Industrial-scale radio frequency treatments for insect control in walnuts. Postharvest Biol. Technol. 45 (2), 240–246.
Wang, S., Monzon, M., Johnson, J.A., Mitcham, E.J., Tang, J., 2007b. Industrial-scale radio frequency treatments for insect control in walnuts. Postharvest Biol. Technol. 45 (2), 247–253.
Wang, S., Tang, J., Sun, T., Mitcham, E.J., Koral, T., Birla, S.L., 2006. Considerations in design of commercial radio frequency treatments for postharvest pest control in in-shell walnuts. J. Food Eng. 77 (2), 304–312.
Wang, S., Yue, J., Chen, B., Tang, J., 2008. Treatment design of radio frequency heating based on insect control and product quality. Postharvest Biol. Technol. 49 (3), 417–423.
Wang, S., Yue, J., Tang, J., Chen, B., 2005. Mathematical modelling of heating uniformity for in-shell walnuts subjected to radio frequency treatments with intermittent stirrings. Postharvest Biol. Technol. 35 (1), 97–107.
Zhu, H., Huang, Z., Wang, S., 2014. Experimental and simulated top electrode voltage in free-running oscillator radio frequency systems. J. Electromag. Waves Appl. 28 (5), 606–617.